Comparison of the dehalogenation of polyhalomethanes and production of strong acids in aqueous and salt (NaCl) water environments: Ultraviolet photolysis of CH₂I₂

Xiangguo Guan, Yong Du, Yun-Liang Li, Wai Ming Kwok, and David Lee Phillips[a]
Department of Chemistry, University of Hong Kong, Pokfulam Road, Hong Kong,
People's Republic of China

The ultraviolet photolysis of CH_2I_2 was studied in water and salt water solutions using photochemistry and picosecond time-resolved resonance Raman spectroscopy. Photolysis in both types of environments produces mainly $CH_2(OH)_2$ and HI products. However, photolysis of CH_2I_2 in salt water leads to the formation of different products/intermediates (CH_2ICl and Cl_2^-) not observed in the absence of salt in aqueous solutions. The amount of $CH_2(OH)_2$ and HI products appears to decrease after photolysis of CH_2I_2 in salt water compared to pure water. We briefly discuss possible implications of these results for photolysis of CH_2I_2 and other polyhalomethanes in sea water and other salt aqueous environments compared to nonsalt water solvated environments. © *2004 American Institute of Physics.* [DOI: 10.1063/1.1803508]

I. INTRODUCTION

The photochemistry and chemistry of a range of polyhalomethnaes such as CH_2I_2, CH_2BrI, $CHBr_3$, CCl_4, $CFCl_3$, and others have been observed in the atmosphere and are important sources of reactive halogens in the natural environments.[1–8] The photochemistry of CH_2I_2 and CH_2BrI have been linked to the production of IO during localized ozone-depletion events in the marine boundary layer of the troposphere.[7,8] The photochemistry of CH_2I_2 was also recently linked to the formation of iodine aerosols although the mechanism for formation remains unclear.[9] Both gas and condensed phase photochemistry and chemistry are important for describing chemical reaction processes in the natural environment.[9–21] Reactions relevant to the activation of halogens in aqueous sea-salt particles have received much interest.[9–21] Recent experiments have found that the water dimer is present at 294 K and it was suggested that larger water clusters (with $n = 3–6$) may also exist in amounts comparable to ambient aerosol in the background troposphere.[22] A theoretical investigation employing complete basis set-atomic pair natural orbit basis set atomic (CBS-APNO) free energies to estimate the number of higher order water clusters found excellent agreement between a predicted calculated concentration of 4×10^{14} water dimers/cm³ compared to the experimental value of 6×10^{14} water dimers/cm³ at a temperature of 292.4 K.[22,23]

Ultraviolet photolysis of polyhalomethanes in the gas phase typically results in one direct carbon-halogen bond scission reaction to produce halomethyl radical and halogen atom fragments.[24–40] In condensed phase environments, these initially produced photofragments can undergo solvent induced geminate recombination to form appreciable amounts of isopolyhalomethanes.[41–59] We have recently investigated the chemical reactivity of isopolyhalomethanes

both theoretically and experimentally and found they are carbenoid species that can react with C=C bonds in olefins to produce cyclopropanated products and a halogen molecule leaving group.[54,55,60–67] The experimental and theoretical results for the isodiiodomethane species indicated that it is probably the predominant carbenoid responsible for the cyclopropanation of olefins when employing the method of ultraviolet photolysis of CH_2I_2 and a reaction mechanism was proposed.[60–62,65,67] Other isopolyhalomethanes were also found to be able to undergo similar reactions with C=C bonds of olefins.[54,55,63,64,67]

Carbenoids and carbenes such as singlet methylene and dichlorocarbene can also react via O–H insertion reactions with the O–H bonds of water and alcohols.[68–77] For example, the reactions of singlet methylene and dichlorocarbene with water give CH_3OH and $CHCl_2OH$ products, respectively.[68–77] We have recently used picosecond time-resolved resonance Raman (ps-TR³) experiments to directly observe the reaction of isobromoform with water to produce a $CHBr_2OH$ product species.[78,79] This indicates isopolyhalomethanes are also able to react with water to make halogenated methanol products.[78,79] A recent study of the ultraviolet photolysis of low concentrations of CH_2I_2 in water found that this resulted in almost complete conversion into $CH_2(OH)_2$ and 2HI products.[80] Ps-TR³ spectra in mixed aqueous solvents (25% to 75% water) found appreciable amounts of isodiiodomethane ($CH_2I–I$) were produced within several picoseconds and its decay became significantly faster with increasing water concentration suggesting the $CH_2I–I$ species could be reacting with water. *Ab initio* calculations indicate the $CH_2I–I$ species reacts readily with water via a water catalyzed O–H insertion/HI elimination reaction followed by its CH_2IOH product decaying via a water catalyzed HI elimination reaction to produce a formaldehyde product that further reacts with water to produce the

methanediol $[CH_2(OH)_2]$ final product observed in the photochemistry experiments.[80]

In this paper, we investigate the photochemistry of CH_2I_2 in salt water environments and compare these results to those previously found in pure water and/or water/acetonitrile mixed solvents. These results should help better understand the photochemistry of CH_2I_2 and other polyhalomethanes found in sea water in the marine boundary layer. Photochemistry and time-resolved resonance Raman experiments indicate that the Cl^- ions from salt (NaCl) can scavenge some of the initial CH_2I and I photofragments produced after ultraviolet photolysis of the parent CH_2I_2 molecule to make Cl_2^- and CH_2ClI products/intermediates. However, there is still substantial solvent induced geminate recombination of the initial photofragments to make isodiiodomethane that then reacts with water to eventually produce $CH_2(OH)_2$ and HI products. We briefly discuss the likely implications for the phase dependent photochemistry of CH_2I_2 and other polyhalomethanes in different natural environments that contain substantial quantities of saltlike sea water and aqueous sea-salt particles and those that contain little or no saltlike fresh water droplets and/or ice particles.

II. EXPERIMENTAL DETAILS

A. Photochemistry experiments

Sample solutions were prepared using commercially available CH_2I_2 (99%), $^{13}CH_2I_2$, formaldehyde in water (reagent grade), D_2O 99.9% D, de-ionized water, and NaCl. Samples of about $(1\times10^{-4})M$ CH_2I_2 in water and $0.5M$ NaCl solution were prepared for use in the photochemistry experiments. These sample solutions were put in a 10 cm path length glass holder with quartz windows and excited by an about 3 mJ 266 nm unfocused laser beam from the fourth harmonic of a Nd:YAG (YAG—yttrium aluminum garnet) laser in the photolysis experiments. The absorption spectra for the photolyzed samples were acquired with a 1 cm UV grade cell and a Perkin Elmer Lambda 19 UV/VIS spectrometer. The pH of the photolyzed samples was obtained using a THERMO Orion 420A pH meter using a 8102BN combination electrode that was calibrated with 7.00 pH and 4.01 pH buffer solutions. Both the ^{13}C and ^1H NMR spectra were acquired using a Bruker Advance 400 DPX spectrometer and $\phi=5$ mm sample tubes at room temperature.

B. Picosecond time-resolved resonance Raman (ps-TR³) spectroscopy experiments

A commercial femtosecond mode-locked Ti: sapphire regenerative amplifier laser was used for the experiments. The output from the laser (800 nm, 1 ps, 1 kHz) was doubled and tripled to by potassium dihydrogen phosphate (KDP) crystals to produce the 400 nm probe and 267 nm pump excitation wavelengths used in the experiments. Fluorescence depletion of *trans*-stilbene was used to determine the time-zero delay between the pump and probe laser beams by varying the optical delay between the pump and probe beams to a position were the depletion of the stilbene fluorescence was halfway to the maximum fluorescence depletion by the probe laser. The time-zero determination was estimated to be accu-

rate to ±0.5 ps and a typical cross correlation time was found to be about 1.5 ps full width at half maximum. The pump and probe laser beams with magic angle polarization were loosely focused onto a flowing liquid stream of sample (about 500 μm thick) with typical pulse energies and spot sizes at the sample of 15 μJ and 250 μm for the pump beam and 8 μJ and 150 μm for the probe beam. A backscattering geometry was used to excite the sample and to collect the Raman scattered light that was then imaged through the entrance slit of a 0.5 m spectrograph. The grating (1200 groove/mm blazed at 250 nm) of the spectrograph dispersed the Raman light onto a liquid nitrogen cooled CCD detector mounted on the exit port of the spectrograph.

Each spectrum shown for our present study was obtained from subtraction of scaled probe-before-pump and scaled net solvent measurements from a pump-probe spectrum in order to remove the ground state CH_2I_2 Raman bands and residual solvent Raman bands, respectively. The known Raman shifts of the solvent Raman bands were employed to calibrate the spectra with an estimated uncertainty of ±5 cm^{-1} in absolute frequency. Commercially available 99% CH_2I_2, spectroscopic grade acetonitrile, and NaCl were used to prepare half liter volume CH_2I_2 ($7\times10^{-3}M$) sample solutions with varying salt concentrations ($0M$, $0.2M$, and $0.5M$ NaCl) and water concentrations (0%, 25%, 50% and 75% water by volume). The samples showed less than a few percent decomposition during the experiments as determined from UV/VIS spectra taken before and after the ps-TR³ measurements.

C. Nanosecond time-resolved resonance Raman (ns-TR³) spectroscopy experiments

The ns-TR³ experimental apparatus and methods have been detailed previously[62,64,65] so only a short description will be given here. The ns-TR³ experiments employed two Nd:YAG lasers that were electronically synchronized via a pulse delay generator to control the relative timing of their flashlamps and Q switches. The relative timing of the 266 nm pump and 255 nm probe laser pulses was monitored using a fast photodiode whose output was displayed on a 500 MHz oscilloscope. The jitter was found to be <5 ns. The laser beams were lightly focused onto a flowing liquid stream of sample using a near collinear geometry and the Raman scattered light was acquired using a backscattering geometry. The Raman light was then imaged through a depolarizer and entrance slit of a 0.5 m spectrograph and dispersed by a grating onto a liquid nitrogen cooled CCD detector mounted on the exit of the spectrograph. The Raman signal was accumulated for about 300 to 600 s by the CCD detector before being read out to an interfaced PC computer. About 10–20 of these readouts were summed to obtain a resonance Raman spectrum. Pump-only, probe-only, and pump-probe resonance Raman spectra were acquired as well as a background scan. The probe-only spectrum was subtracted from the pump-probe spectrum to remove precursor and solvent Raman bands, and then the pump-only spectrum and background scan were also subtracted in order to obtain the time-resolved resonance Raman spectrum.

The known Raman shifts of the solvent Raman bands were used to calibrate the spectra with an estimated uncer-
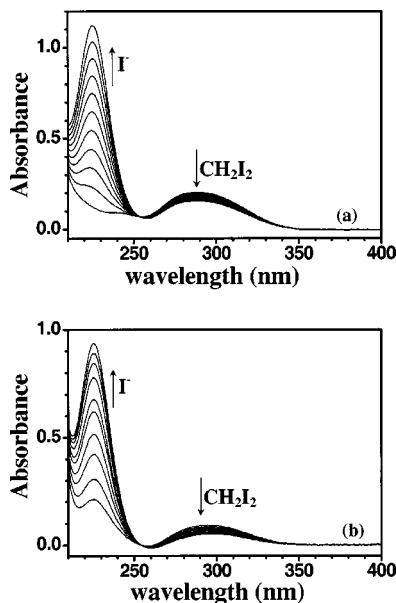
FIG. 1. Absorption spectra obtained after different 266 nm photolysis times of $1 \times 10^{-4} M$ CH$_2$I$_2$ in pure water (a) and in 0.5M NaCl aqueous solution (b). The parent CH$_2$I$_2$ absorption bands in the 280–320 nm region decrease in intensity as a new absorption band due to I$^-$ appears at about 225 nm with a clear isobestic point at 253 nm. The I$^-$ absorption band is essentially identical to that found for KI salt dissolved in water and NaCl solutions.

tainty of ± 5 cm^{-1} in absolute frequency. Commercially available K$_2$S$_2$O$_8$ and NaCl 99% were used to prepare a sample solution. This sample with 0.05M K$_2$S$_2$O$_8$ and 0.5M NaCl in a 75% water/25% acetonitrile solution was photolyzed to produce an authentic Cl$_2^-$ ns-TR^3 spectrum using a method similar to that described by Hynes and Wine in Ref. 81. Commercially available 99% CH$_2$I$_2$ and I$_2$ and spectroscopic grade acetonitrile and NaCl were used to prepare half liter volume CH$_2$I$_2[(1 \times 10^{-2})M]$ and I$_2[(2 \times 10^{-3})M]$ sample solutions with 0.5M NaCl in a 75% water/25% acetonitrile by volume solvent. UV/VIS spectra taken before and after the ns-TR^3 measurements indicated the samples showed less than a few percent decomposition over the experiments.

III. RESULTS AND DISCUSSION

A. Product analysis of CH$_2$I$_2$ ultraviolet photolysis in water and salt water

Figure 1 shows ultraviolet/visible spectra acquired following photolysis for varying times using 266 nm laser excitation of a $(1 \times 10^{-4})M$ CH$_2$I$_2$ sample in pure water (A) and in salt water solution (0.5M NaCl) (B). Examination of Fig. 1 reveals that in both cases the absorption bands due to CH$_2$I$_2$ in the 280–320 nm region decrease in intensity while those due to the I$^-$ ion in the 225 nm region increase in intensity as the time for photolysis increases. Inspection of Fig. 1 shows there is a clear isobestic point at around 253 nm indicating the I$^-$ is directly produced from the CH$_2$I$_2$ parent molecule. The pH of the sample solutions was also measured at the same time the absorption spectra were acquired. The molar extinction coefficients for CH$_2$I$_2$ and I$^-$ were used to find the concentrations of these species for each of the pho-
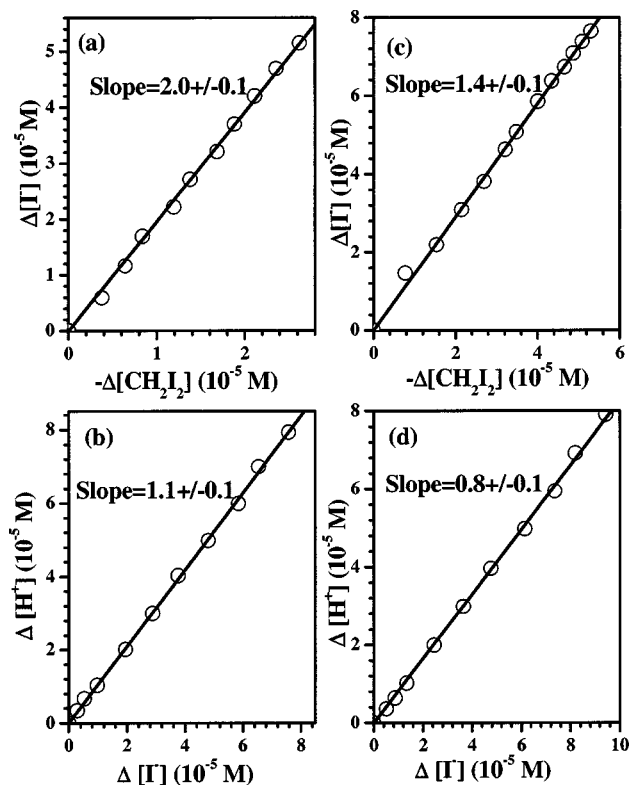

FIG. 2. Plots of $\Delta[$I$^-]$ vs $-\Delta[$CH$_2$I$_2]$ derived from the absorption spectra shown in Fig. 1 are given for experiments done in pure water solvent (a) and in 0.5M NaCl salt water solvent (c). Plots of $\Delta[$H$^+]$ obtained from the pH measurements vs $\Delta[$I$^-]$ from the absorption spectra of Fig. 1 are presented for experiments done in pure water solution (b) and in 0.5M NaCl salt water solvent (d). Best fits of the data to a linear regression are shown as lines with the slopes of the lines indicated next to the lines. See text for more details.

tolysis times from the UV/VIS spectra presented in Fig. 1 and the change in the concentration of H$^+$ was determined from the pH measurements. Plots of $\Delta[$I$^-]$ versus $-\Delta[$CH$_2$I$_2]$ during the photochemistry experiments were made and are presented in (a) and (c) of Fig. 2. The increase in [I$^-$] versus the decrease in [CH$_2$I$_2$] during the photochemistry experiments reveals a linear relationship with a slope of about 2 for the experiments done in pure water solvent and a slope of about 1.4 in the salt water (0.5M NaCl) solvent. These results indicate that ultraviolet photolysis of CH$_2$I$_2$ at low concentrations in water and salt water (0.5M NaCl) solvents releases about 2I$^-$ and 1.4I$^-$ final products, respectively. Plots of the changes in the [H$^+$] concentrations found from the pH measurements were plotted versus the changes in the [I$^-$] concentrations and these are given in (b) and (d) of Fig. 2. The plots of $\Delta[$H$^+]$ versus $\Delta[$I$^-]$ have linear correlation and slopes of about 1 and 0.8, respectively for CH$_2$I$_2$ photolysis in pure water and in salt water (0.5M NaCl), respectively. The preceding results from the UV/VIS and pH photochemistry experiments presented in Figs. 1 and 2 indicate that photolysis of low concentrations of CH$_2$I$_2$ produces 2H$^+$ and 2I$^-$ products in pure water and about 1.15H$^+$ and 1.4I$^-$ products in the 0.5M NaCl salt water solvent. Most of the H$^+$ and I$^-$ products formed are probably from HI leaving group(s) that dissociate into H$^+$ and I$^-$ in the aqueous solvents.
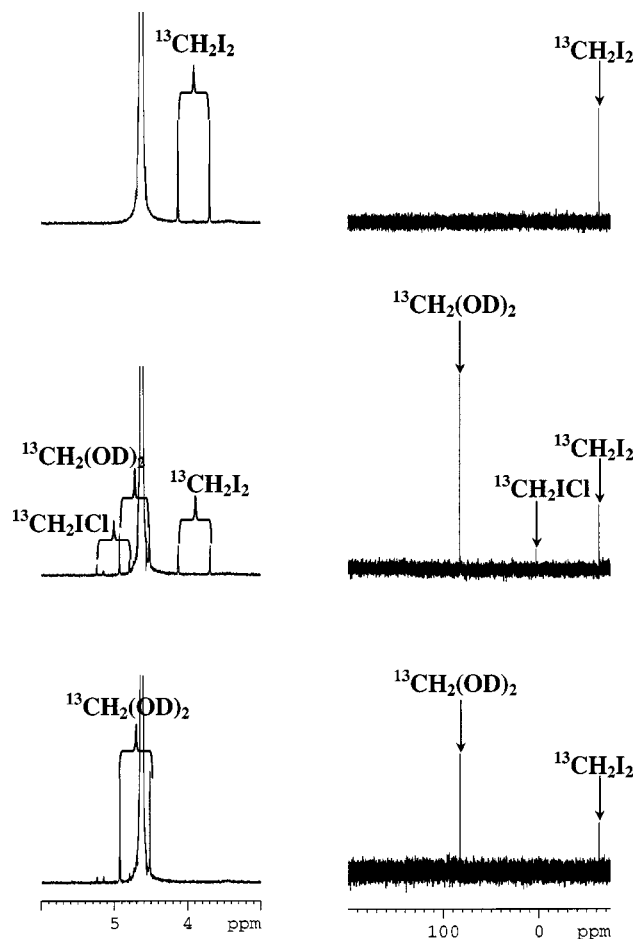
FIG. 3. ^{1}H-NMR spectra (left column) and ^{13}C-NMR spectra (right column) obtained before (top), during (middle) and after complete (bottom) 266 nm photolysis of ^{13}CH$_2$I$_2$ in 0.5M NaCl D$_2$O solution. The parent CH$_2$I$_2$ band appears at about 3.9 ppm in the ^{1}H-NMR spectra and about -63.9 ppm in the ^{13}C-NMR spectra. Photolysis converts the ^{13}CH$_2$I$_2$ parent band into mainly photoproduct assigned to ^{13}CH$_2$(OD)$_2$ that has a doublet around 4.7 ppm in the ^{1}H-NMR spectra and a singlet at 82.5 ppm in the ^{13}C-NMR spectra. Another minor product is observed as a doublet around 5.0 ppm in the ^{1}H-NMR spectra and about 2.8 ppm in the ^{13}C-NMR spectra assigned to CH$_2$ICl. See text for more details.
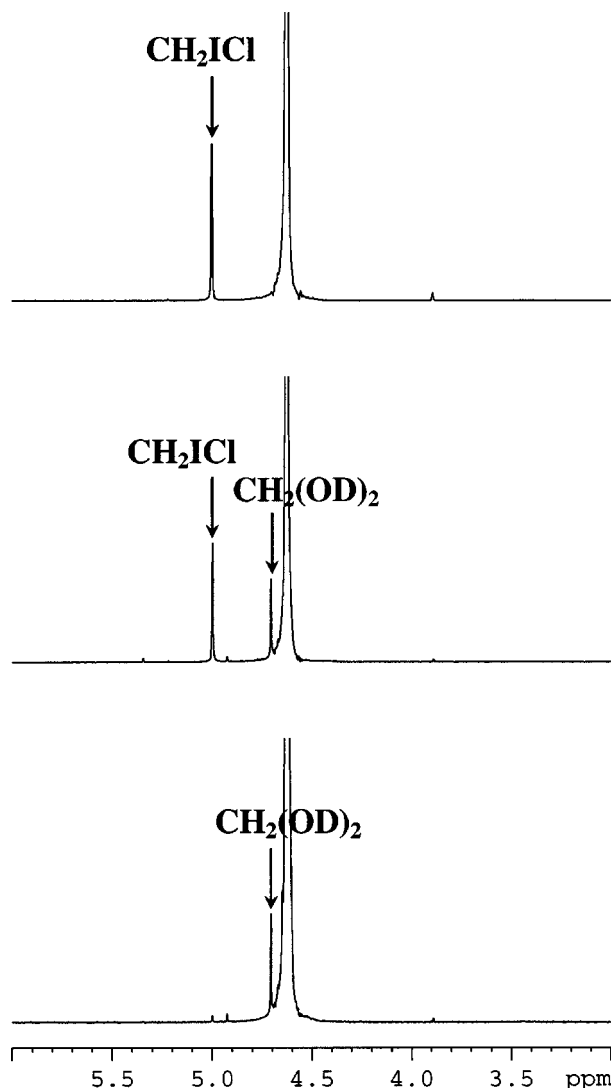

FIG. 4. ^{1}H-NMR spectra obtained before (top), during (middle) and after complete (bottom) 266 nm photolysis of CH$_2$ICl in D$_2$O solution. Photolysis of CH$_2$ICl converts the parent band into a methanediol product [CH$_2$(OD)$_2$]. See text for more details.

To learn more about the fate of the carbon atom from the CH$_2$I$_2$ parent molecule after ultraviolet photolysis in the salt water (0.5M NaCl) solvent, we employed a carbon-13 labeled sample of CH$_2$I$_2$. We then repeated the ultraviolet photolysis experiments given in Figs. 1 and 2 and obtained ^{1}H-NMR and ^{13}C-NMR spectra before, during, and after complete photolysis of ^{13}CH$_2$I$_2$ in D$_2$O salt water (0.5M NaCl) solvent as shown Fig. 3. Spectra obtained in the pure water solvent were essentially the same as that reported in Ref. 80 and the reader is referred to Figs. 1 and 3 for the ^{1}H-NMR and ^{13}C-NMR spectra in Ref. 80 for the spectra found for photolysis of CH$_2$I$_2$ in pure water. The ^{1}H-NMR and ^{13}C-NMR bands due to the parent ^{13}CH$_2$I$_2$ (3.9 and -63.9 ppm, respectively) are labeled in Fig. 3 and upon photolysis these bands become noticeably smaller and new bands due to ^{13}CH$_2$(OD)$_2$ (doublet around 4.7 ppm and 82.5 ppm, respectively) and ^{13}CH$_2$ICl (doublet around 5 and 2.8 ppm, respectively) were produced (see middle spectra of Fig. 3). The assignment of spectral bands for the ^{13}CH$_2$(OD)$_2$

and ^{13}CH$_2$ICl products were confirmed by comparison to spectra of authentic samples of methandiol and CH$_2$ICl. Further ultraviolet photolysis appears to also convert the ^{13}CH$_2$ICl product into ^{13}CH$_2$(OD)$_2$ (see bottom spectra of Fig. 3). This prompted us to also do an analogous photochemistry experiment using CH$_2$ICl in pure D$_2$O solvent and taking ^{1}H-NMR spectra before, during, and after 266 nm photolysis as shown in Fig. 4. Inspection of Fig. 4 shows that ultraviolet photolysis of CH$_2$ICl in pure D$_2$O appears to produce methandiol [CH$_2$(OD)$_2$] product and these results are consistent with those we found in the photolysis of CH$_2$I$_2$ in salt water as shown in Fig. 3.

The preceding experimental photochemistry results suggest that the main reaction occurring after ultraviolet photolysis of low concentrations of CH$_2$I$_2$ in pure water and salt water leads to the following overall reaction:

$$CH_2I_2 + h\nu + nH_2O \rightarrow CH_2(OH)_2 + 2HI + (n-2)H_2O. \tag{1}$$
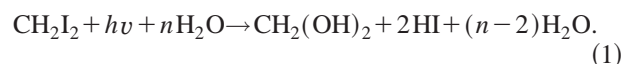
However, in the salt water solution this reaction is not the only significant one and the formation of the CH_2ICl product lowers the amount of formation of both the $CH_2(OH)_2$ and HI products which indicates another reaction is competing with the main overall reaction given in Eq. (1).

We note that photochemistry experiments done with an unfocused nanosecond laser beam and a Hg lamp source of light resulted in essentially the same results for the production of the products for low concentrations of CH_2I_2 in water and salt water. The reader is referred to Ref. 80 for a comparison of the laser photolysis and the Hg photolysis experiments in pure water. This indicates the photoproducts observed in Figs. 1–4 are produced mainly from one-photon excitation of CH_2I_2.

To help better understand how the ultraviolet photolysis of CH_2I_2 in salt water leads to mainly formation of methandiol $[CH_2(OH)_2]$ and HI products accompanied by CH_2ICl product, we have done additional picosecond and nanosecond time-resolved resonance Raman (ps-TR[3] and ns-TR[3], respectively) experiments in salt water environments and compare them to results previous found in pure water. This is detailed in the following section.

B. Picosecond and nanosecond time-resolved resonance raman experiments

Figure 5 shows ps-TR[3] spectra obtained following 267 nm photolysis of CH_2I_2 in H_2O/CH_3CN mixed solvents with different concentrations of NaCl using a 400 nm probe excitation wavelength. Spectra in Figs. 5(a)–5(c) were obtained in $0.0M$, $0.2M$ and $0.5M$ NaCl in 75% H_2O/25% CH_3CN solution, respectively. Spectra in Figs. 5(d) and 5(e) were obtained using the same NaCl concentration ($0.2M$) with different water concentrations of 50% H_2O/50% CH_3CN and 75% H_2O/25% CH_3CN solutions, respectively. The Raman bands observed for the first photoproduct species (from several picoseconds to several hundred picoseconds) are straight forward to assign to the isodiiodomethane (CH_2I–I) species and the reader is referred to Refs. 49, 52, and 59 for details of the assignment.

Inspection of Fig. 5 shows that the CH_2I–I photoproduct Raman bands appear within several picoseconds and then decay on the hundreds of picosecond to nanosecond time scale. As the salt concentration increases in Figs. 5(b) and 5(c) new photoproduct bands appear in the 500 ps to 5000 ps time scale that are not found in the spectra obtained in pure water (a). The new photoproduct Raman bands only appear in the presence of appreciable amounts of NaCl in the aqueous solution. Examination of the ps-TR[3] spectra in Figs. 5(d) and 5(e) obtained at the same salt concentration ($0.2M$ NaCl) but with different water concentrations (with 50% H_2O and 75% H_2O, respectively) reveals that the new photoproduct Raman bands appear the same at 5000 ps. However, the decay of the CH_2I–I species becomes substantially faster at higher H_2O concentration and indicates that the CH_2I–I species reacts with H_2O. The results shown in Figs. 5(d) and 5(e) indicate the decay of the CH_2I–I species is not linked to the growth of the new photoproduct species Raman bands observed at 5000 ps and some other reaction is responsible for these bands.
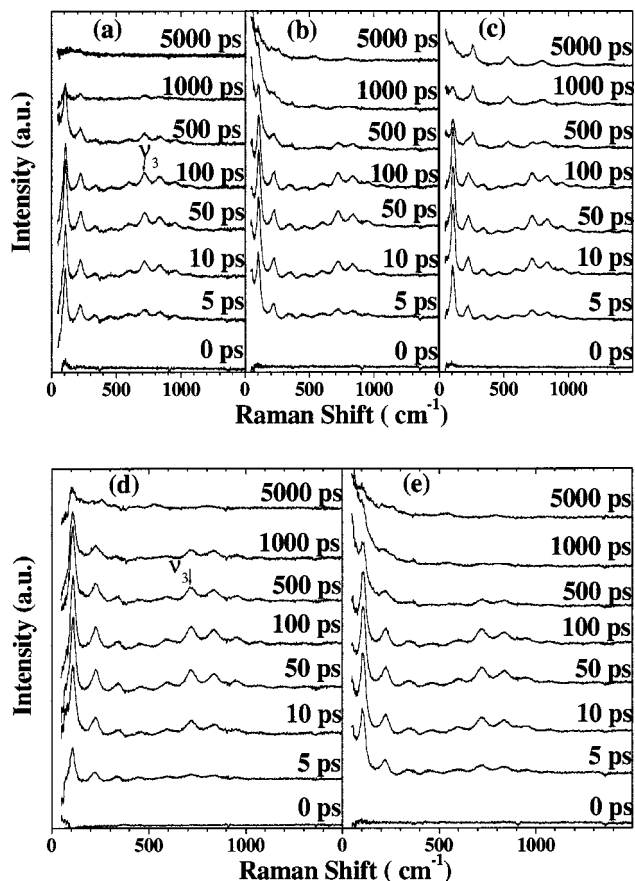

FIG. 5. Stokes ps-TR[3] spectra (using a 400 nm probe excitation wavelength) obtained following 267 nm photolysis of CH_2I_2 in H_2O/CH_3CN mixed solvents with different NaCl and/or water concentrations. Spectra in (a), (b), and (c) were acquired in $0.0M$, $0.2M$ and $0.5M$ NaCl in 75% H_2O/25% CH_3CN solutions respectively. Spectra in (d) and (e) were obtained using the same salt concentration ($0.2M$ NaCl) and different concentrations of water, 50% H_2O/50% CH_3CN and 75% H_2O/25% CH_3CN solutions, respectively.

The CH_2I–I Raman band near 715 cm^{-1} assigned to the fundamental C–I stretch mode (v_3) was integrated at different time delays so as to determine the kinetics of the growth and decay of the CH_2I–I species. Figure 6 (top) presents plots of the relative integrated area of the v_3 Raman band from 0 to 3000 ps in the $0.0M$ (solid square), $0.2M$ (solid star) and $0.5M$ (open triangle) NaCl in 75% H_2O/25% CH_3CN mixed solutions. Figure 6 (bottom) shows plots of the relative integrated area of the v_3 Raman band from 0 ps to 6000 ps in the $0.2M$ NaCl in 50% H_2O/50% CH_3CN (solid triangle) and 75% H_2O/25% CH_3CN (solid star) mixed solutions. The relative integrated areas of the v_3 Raman bands were fit to a simple function $I(t) = Ae^{-t/t1} - Be^{-t/t2}$ (dashed lines in Fig. 6 represent these fits), where $I(t)$ is the relative integrated area of the v_3 Raman band, t is the time, t_1 is the decay time constant of the v_3 Raman band, t_2 is the growth time constant of the v_3 Raman band, and A and B are constants. The fits to the data in the top of Fig. 6 found the CH_2I–I species had growth time constants t_2 of about 6, 7, and 7 ps, and decay time constants t_1 of about 650, 480, and 430 ps for the $0.0M$, $0.2M$ and $0.5M$ NaCl in 75% H_2O/25% CH_3CN so-
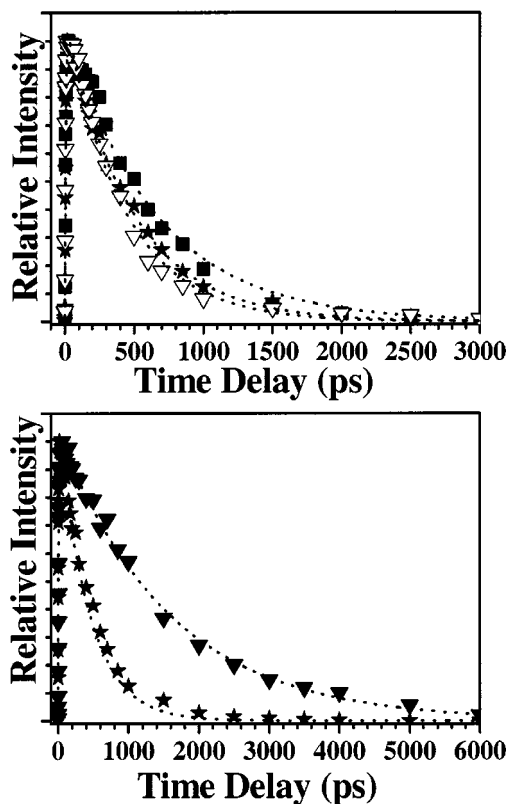
FIG. 6. (Top) Plots of the relative integrated area of the v_3 Raman band of CH$_2$I–I at different delay times (from 0 to 3,000 ps) obtained from the spectra of Figs. 5(a)–5(d) in 75% H$_2$O/25% CH$_3$CN solutions with different concentrations of NaCl: 0.0M NaCl (solid square), 0.2M NaCl (solid star) and 0.5M NaCl (open triangle). The dotted lines represent least square fits to the data (see text for more details). (Bottom) Plots of the relative integrated area of the v_3 Raman band of CH$_2$I–I at different delay times (from 0 to 6000 ps) obtained from the spectra of Figs. 5(d) and 5(e) with the same 0.2M NaCl but with different concentrations of H$_2$O: 50% H$_2$O/50% CH$_3$CN (solid triangle) and 75% H$_2$O/25% CH$_3$CN (solid star). The dotted lines represent least square fits to the data (see text for more details).

FIG. 7. Comparison of Stokes ps-TR^3 spectra obtained following 267 nm photolysis of I$_2$ (a) and CH$_2$I$_2$ (b) in solutions of 0.5M NaCl in 75% H$_2$O/25% CH$_3$CN solvent. See text for more details.

lutions, respectively. The fits to the data at the bottom of Fig. 6 found the CH$_2$I–I species had growth time constants t_2 of about 10 ps and 7 ps and decay time constants t_1 of about 1580 ps and 480 ps for the 0.2M NaCl in 50% H$_2$O/50% CH$_3$CN and 75% H$_2$O/25% CH$_3$CN solutions, respectively.

The growth time constants for the CH$_2$I–I species are very similar in the different water and salt concentrations (all in the 6–10 ps range) and consistent with its formation by some solvent induced geminate recombination of the initially produced CH$_2$I radical and I atom photofragments as has been found previously in organic solvents and in mixed water solvents.[45,49,59,80] The decay of the CH$_2$I–I species in salt water solutions with varying concentrations of salt becomes only moderately faster with increasing salt concentration (time constants of about 480 ps for 0.2M NaCl and 430 ps for 0.5M NaCl). The CH$_2$I–I species has appreciable radical ion pair character (e.g., such as CH$_2$I$^+$I$^-$) which would be expected to be perturbed by a changing solvent polarity or dielectric properties. Thus, the modest changes in the CH$_2$I–I decay time in different salt concentrations can probably be attributed to a moderate change in the stability of

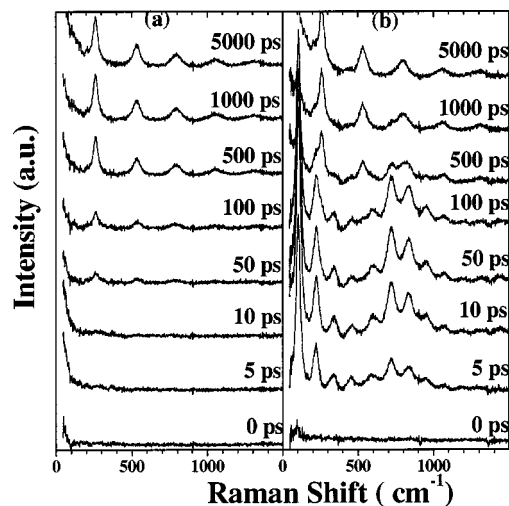the CH$_2$I–I species in the salt solutions rather than some reaction with NaCl. This is consistent with previous observations that the lifetime of CH$_2$I–I does vary noticeably with the polarity of the solvent[59,82] and the lack of any correlation of the CH$_2$I–I decay time with the appearance time of the second product species observed at longer delay times. The decay of the CH$_2$I–I species changes substantially with the concentration of H$_2$O (from 1580 ps in 0.2M NaCl 50% H$_2$O/50% CH$_3$CN to 480 ps in 0.2M NaCl 75% H$_2$O/25% CH$_3$CN solutions). This is very similar to the behavior of CH$_2$I–I as the concentration of H$_2$O increases in mixed aqueous solvents in the absence of NaCl where the decay times were found to be about 1860 ps in 50% H$_2$O/50% CH$_3$CN and 680 ps in 75% H$_2$O/25% CH$_3$CN solutions.[59,80] This significantly faster decay of the CH$_2$I–I species as the water concentration increases was attributed to an O–H insertion reaction of CH$_2$I–I with H$_2$O.[80,83] We observe almost identical behavior in the salt water solutions investigated here and similarly attribute this to the O–H insertion reaction of the CH$_2$I–I carbenoid species with H$_2$O as deduced in Ref. 80.

One of the photoproducts observed in the salt water photochemistry experiments is CH$_2$ICl and this species is not observed in the nonsalt water photochemistry experiments. One possibility for the formation of the CH$_2$ICl product could be reaction of the initially formed CH$_2$I radical photofragment with a nearby NaCl. If this occurs then one could expect the other I atom photofragment could be readily scavenged by Cl$^-$ ions from NaCl as well. Therefore, we performed 267 nm pump and 400 nm probe ps-TR^3 experiments with I$_2$ in a 0.5M NaCl 75% H$_2$O/25% CH$_3$CN solution and compared this to the analogous experiment for CH$_2$I$_2$ and these spectra are shown in Fig. 7. Ultraviolet (267 nm) photolysis of I$_2$ would be expected to produce two I atom photofragments and it would be reasonable to expect that some of these may directly react with NaCl on the picosecond to nanosecond time scale. This is precisely what is observed in the ps-TR^3 spectra obtained after photolysis of I$_2$ in 0.5M
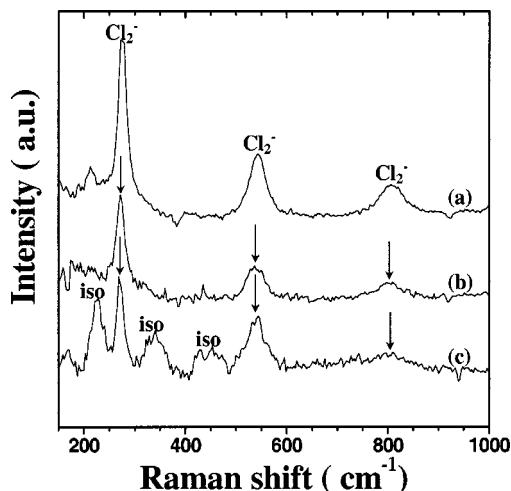
FIG. 8. Nanosecond time-resolved resonance Raman (ns-TR^3) spectra of Cl$_2^-$ produced from photolysis of persulphate in the presence of Cl$^-$ ions (a) and photoproducts produced after 266 nm photolysis of I$_2$ (b) and CH$_2$I$_2$ (c) in 0.5M NaCl 75% water/25% acetonitrile solution. The spectra were obtained with a 355 nm probe wavelength and about 5–10 ns after the 266 nm pump laser pulse. The resonance Raman bands due mainly to the isodiiodomethane photoproduct bands in spectrum (c) have been labeled with "iso". See text for more details.

NaCl 75% H$_2$O/25% CH$_3$CN solution. The fundamental vibrational frequency of 265 cm^{-1} observed for the predominant progression of the photoproduct is in good agreement with the 271–273 cm^{-1} observed previously for the Cl$_2^-$ time-resolved resonance Raman spectrum with 355 nm or 359 nm excitation.[81,84,85] In the TR^3 experiments of Tripathi, Schuler, and Fessenden,[85] the Cl$_2^-$ and other dihalides such as Br$_2^-$ and I$_2^-$ were produced by OH oxidation of the halide,

$$OH + X^- \rightarrow X + OH^-, \tag{2}$$

$$X + X^- \rightarrow X_2^-, \quad \text{where} \quad X = Cl, Br, I. \tag{3}$$
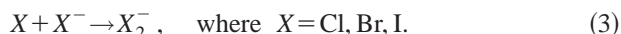
The analogous reactions for I atoms with NaCl would be the following:

$$I + Na^+Cl^- \rightarrow Cl + Na^+I^-, \tag{4}$$

$$Cl + Cl^- \rightarrow Cl_2^-. \tag{5}$$

However, the I/I$^-$ one electron redox potential in water is ≈ 1.3 eV while the Cl/Cl$^-$ one electron redox potential in water is ≈ 2.4 eV and this makes the overall reaction I $+ Cl^- \rightarrow Cl + I^-$ endothermic by about 1.1 eV. This indicates the I$+Cl^- \rightarrow Cl+I^-$ reaction should not occur at an appreciable rate and thus is inconsistent with the fast formation observed in the ps-TR^3 experiments. Therefore, some other mechanism than that given by Eqs. (4) and (5) must be responsible for the formation of Cl$_2^-$.

We performed additional ns-TR^3 experiments to produce an authentic Cl$_2^-$ resonance Raman spectrum based on another known method of photolysis of persulphate in the presence of Cl$^-$ ions similar to that done by Hynes and Wine in Ref. 81. At the same time we obtained spectra at about 5–10 ns after photolysis of samples of I$_2$ and CH$_2$I$_2$ in 0.5M NaCl in 75% water/25% acetonitrile solvent. These ns-TR^3 spectra are shown in Fig. 8. Figure 8(a) displays the Cl$_2^-$ ns-TR^3

spectrum generated by photolysis of persulphate in the presence of Cl$^-$ ions. This resonance Raman spectrum is in excellent agreement with that previously reported by Hynes and Wine using a similar method in Ref. 81. The Raman band shifts for the first three bands in Fig. 8(a) are about 275 cm^{-1}, 542 cm^{-1}, and 808 cm^{-1} and these are in excellent agreement with those of 273$\pm$2 cm^{-1}, 543$\pm$2 cm^{-1}, 808$\pm$2 cm^{-1} reported in Ref. 81. Thus, we are confident the spectrum shown in Fig. 8(a) is due to the Cl$_2^-$ species. Comparison of this Cl$_2^-$ resonance Raman spectra [Fig. 8(a)] to those obtained at about 5–10 ns after 266 nm photolysis of I$_2$ and CH$_2$I$_2$ in a 0.5M NaCl 75% water/25% acetonitrile solvent shows that essentially the same resonance Raman bands are found in both cases. This indicates Cl$_2^-$ is also produced after photolysis of I$_2$ and CH$_2$I$_2$ in a 0.5M NaCl 75% water/25% acetonitrile solvent. In the spectrum shown in Fig. 8(c), some isodiiodomethane resonance Raman bands (labeled by iso) are also present similar to the 400 nm ps-TR^3 spectra shown in Figs. 5 and 7.

The ps-TR^3 spectra in Fig. 7 obtained after photolysis of I$_2$ in 0.5M NaCl 75% H$_2$O/25% CH$_3$CN solution is almost identical to that shown in the ns-TR^3 experiments shown in Fig. 8 and those previously observed for Cl$_2^-$ in Refs. 81, 84, and 85. Thus, the product bands that form on the hundreds of picoseconds to nanoseconds time scale in the ps-TR^3 spectra in Fig. 7 acquired after photolysis of I$_2$ in 0.5M NaCl 75% H$_2$O/25% CH$_3$CN solution are assigned to the Cl$_2^-$ species. The ps-TR^3 spectra for the Cl$_2^-$ species produced from photolysis of I$_2$ in 0.5M NaCl 75% H$_2$O/25% CH$_3$CN solution are essentially identical to the ps-TR^3 spectra of the second photoproduct species observed after 267 nm photolysis of CH$_2$I$_2$ in 0.5M NaCl 75% H$_2$O/25% CH$_3$CN solution. Therefore this second photoproduct species is also assigned to Cl$_2^-$ produced from the reaction of I atoms with NaCl. This is consistent with its ps-TR^3 spectral intensity becoming greater and having a faster appearance time as the concentration of the NaCl increases in the spectra shown in Figs. 7(b) and 7(c).

A possible mechanism that may account for fast formation of Cl$_2^-$ after photolysis of I$_2$ and CH$_2$I$_2$ in NaCl water/acetonitrile mixed solvents could be the following:

$$I + Cl^- \rightarrow ICl^-, \tag{6}$$

$$ICl^- + Cl^- \rightarrow Cl_2^- + I^-. \tag{7}$$

Reaction step (6) would be expected to occur very fast since the I atom could be scavenged by the high concentration of Cl$^-$ in the solution and is forming a new I-Cl$^-$ bond. Reaction step (7) may also be very fast since the Cl$^-$ concentration is very high and it is forming a moderately stronger bond (Cl$_2^-$) than it is breaking (ICl$^-$). Photolysis of I$_2$ in the salt water solutions did not produce any obvious Raman bands due to ICl$^-$ at either the 400 nm or 355 nm probe wavelengths used in the ps-TR^3 and ns-TR^3 spectra shown in Figs. 7 and 8, respectively. This could suggest that ICl$^-$ may be very short lived and not a stable species in the presence of Cl$^-$ ions. It is conceivable that reaction steps (6) and (7) both occur very fast and thus there may not be enough buildup of the ICl$^-$ concentration to see a large signal from this species

in the TR^3 spectra examined thus far. The mechanism in reaction steps (6) and (7) is plausible for the fast formation of Cl_2^- after ultraviolet photolysis of I_2 and CH_2I_2 in NaCl water/acetonitrile mixed solvents, but more experimental and theoretical work needs to be done to clearly establish the actual mechanism of Cl_2^- formation. This should prove an interesting area of investigation for the photolysis of iodoalkanes in salt water environments.

C. Proposed reaction mechanism for the $CH_2I_2+h\nu$ $+n(H_2O)\rightarrow CH_2(OH)_2+2HI+(n-2)H_2O$ overall reaction in water and salt water environments and formation of CH_2ICl and Cl_2^- products in the presence of salt (NaCl)

Based on our present experimental results and other work already available in the literature, we propose the following reaction mechanism for the $CH_2I_2+h\nu+n(H_2O)$ $\rightarrow CH_2(OH)_2+2HI+(n-2)H_2O$ overall reaction that we observe for photolysis of low concentrations of CH_2I_2 in aqueous solutions with and without NaCl present:
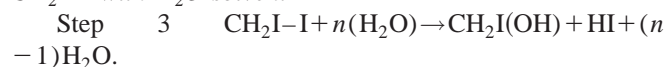
Photolysis of CH_2I_2 to form CH_2I and I fragments
    Step 1 $CH_2I_2+h\nu\rightarrow CH_2I+I$.
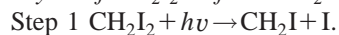
Solvent induced geminate recombination of the CH_2I and I fragments to form the $CH_2I–I$ isomer
    Step 2 $CH_2I+I\rightarrow CH_2I–I$.
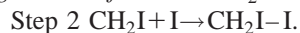
Water-catalyzed O–H insertion/HI elimination reaction of $CH_2I–I$ with H_2O solvent
    Step 3 $CH_2I–I+n(H_2O)\rightarrow CH_2I(OH)+HI+(n-1)H_2O$.

Water-catalyzed HI elimination reaction of $CH_2I(OH)$ with H_2O solvent
    Step 4 $CH_2I(OH)+n(H_2O)\rightarrow H_2CO+HI+n(H_2O)$.

Water (and/or acid) catalyzed addition of H_2O to H_2CO in H_2O solvent
    Step 5 $H_2CO+n(H_2O)\rightarrow CH_2(OH)_2+(n-1)H_2O$.
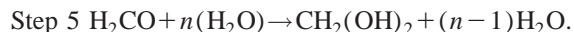
Add steps 1–5 to obtain this overall reaction
    $CH_2I_2+h\nu+n(H_2O)\rightarrow CH_2(OH)_2+2HI+(n-2)H_2O$.

Ultraviolet excitation of CH_2I_2 in both gas and solution phases is known to result in direct cleavage of the C–I bond to produce CH_2I radical and I atom fragments.[24–40,45–48] This indicates step 1 in the above reaction mechanism is the primary photochemical start of the reaction. It has been clearly experimentally shown that some of the initially produced CH_2I radical and I atom fragments undergo solvent induced geminate recombination to form a $CH_2I–I$ isomer species within a few picoseconds.[45,49,59,80,82] This establishes that step 2 of the proposed reaction mechanism occurs to an appreciable degree in room temperature solutions and our present ps-TR^3 spectra in largely aqueous solvents shows this also occurs in water and salt water solutions.

Previous experimental and theoretical work indicate that isopolyhalomethanes such as $CH_2I–I$ are effective carbenoid species that can readily react with C=C bonds in olefins to make cyclopropanated products[54,55,60–67,82] and also undergo O–H insertion reactions with water to produce halogenated methanols.[78–80,83] We have also used ps-TR^3 experiments to directly observe this type of isopolyhalomethane O–H inser-

tion reaction for the isobromoform species reaction with water to form a dibromomethanol ($CHBr_2OH$) reaction product.[78,79] Recent *ab initio* results indicate that $CH_2I–I$ can undergo a water catalyzed O–H insertion/HI elimination reaction with water reasonably easily.[80,83] These previous studies and our present observation of the much faster decay of the $CH_2I–I$ species with increasing water concentration in both nonsalt and salt aqueous solutions indicate that $CH_2I–I$ reacts mainly with water to produce an iodomethanol product and HI leaving group consistent with step 3 of the proposed reaction mechanism.
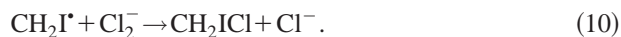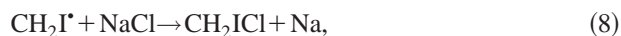
Chloromethanol is known to decompose in the dark to formaldehyde (H_2CO) and HCl products in both the gas phase[86,87] and in the condensed phase (e.g., low temperature matrices).[88] In so far as iodomethanol (CH_2IOH) behaves such as chloromethanol (CH_2ClOH) then one would expect iodomethanol (CH_2IOH) to decay into H_2CO and HI products consistent with step 4 of the proposed reaction mechanism. Recent *ab initio* calculations showed that iodomethanol (CH_2IOH) undergoes a water assisted HI elimination reaction to produce H_2CO and HI products and this provides further support for step 4 of the reaction mechanism.[80] Formaldehyde (H_2CO) is known to react with water to produce methanediol [$CH_2(OH)_2$].[89–91] Thus one would expect the H_2CO product to be efficiently converted to methanediol [$CH_2(OH)_2$] in a water solvated environment consistent with step 5 of the proposed reaction mechanism.

The proposed reaction mechanism given here helps explain how photolysis of low concentrations of CH_2I_2 in aqueous solutions and salt (NaCl) aqueous solutions leads to formation of significant amounts of methanediol [$CH_2(OH)_2$] and HI products that are observed in our ^{13}C-NMR, ^{1}H-NMR, UV/VIS, and pH photochemistry results in both aqueous solutions[80] and salt (NaCl) aqueous solutions (this work, see Figs. 1–3). The proposed reaction mechanism is also consistent with the known photolysis of CH_2I_2 in the gas and solution phases to make CH_2I radical and I photofragments. The reaction mechanism is also consistent with the direct ps-TR^3 observation of the $CH_2I–I$ intermediate and its known chemical reactivity, the known chemistry of halomethanols and the known hydrolysis of H_2CO in aqueous environments.

In salt (NaCl) water solutions, two different products and/or intermediates (CH_2ICl and Cl_2^-) are observed that are not discernible in nonsalt aqueous solutions. This suggests these products is/are produced from some reaction(s) with NaCl. The formation of these products (CH_2ICl and Cl_2^-) in salt aqueous solutions also lower the relative amounts of I^- and H^+ produced per CH_2I_2 molecule photolyzed (see Figs. 1 and 2). This suggests that the amount of the highly reactive $CH_2I–I$ species produced that then further reacts with water to eventually form 2 HI leaving groups may be less in the presence NaCl than in nonsalt aqueous solutions.

It is conceivable that reactions of NaCl with the initially produced CH_2I radical and I atom from the ultraviolet photolysis of the CH_2I_2 molecule can account for both a lower yield of the very reactive isodiiodomethane ($CH_2I–I$) intermediate and the formation of the different CH_2ICl and Cl_2^- products. For example, the reaction of I atoms with Cl^- via

reaction (6) to make an ICl^- product where the ICl^- subsequently reacts with a Cl^- ion via reaction (7) to make the Cl_2^- species can possibly explain the formation of the Cl_2^- species. The Cl_2^- species was observed in the TR^3 experiments (see Figs. 7 and 8 as well as the discussion of the last part of Sec. III B). Similarly, the formation of the CH_2ICl product observed in the NMR photochemistry experiments (see Fig. 3) can conceivably be produced from one or more of the following reactions of CH_2I radicals with species known to be present in the system $(NaCl, Cl^-, Cl_2^-)$:

$$CH_2I^\bullet + NaCl \rightarrow CH_2ICl + Na, \tag{8}$$

$$CH_2I^\bullet + Cl^- \rightarrow CH_2ICl + e^-, \tag{9}$$

$$CH_2I^\bullet + Cl_2^- \rightarrow CH_2ICl + Cl^-. \tag{10}$$

Using our present 400 nm probe wavelength, we could not directly follow the decay of the CH_2I radical nor the formation of the CH_2ICl species in the ps-TR^3 experiments since both species do not absorb appreciably at this wavelength. Thus, we cannot clearly establish the most likely reaction for the formation of the CH_2ICl species. However, it is very likely that one of the reactions of a CH_2I radical with species known to be present in the salt water reaction system produces the CH_2ICl products observed in the NMR photochemistry experiments of Fig. 3. We note that reaction (10) $[CH_2I^\bullet + Cl_2^- \rightarrow CH_2ICl + Cl^-]$ is quite similar to the $Cl^\bullet + Cl_2^- \rightarrow Cl_2 + Cl^-$ reaction in aqueous solution recently studied by Barker and co-workers.[92] In both reactions, a radical (either CH_2I or Cl) reacts with the Cl_2^- species to break its bond and produce a new bond in the neutral species (CH_2ClI or Cl_2) product and a halogen ion leaving group (I^- or Cl^-). One may expect the CH_2I radical reaction may occur more easily since it is forming a stronger bond (C–Cl bond in CH_2ClI) than in the reaction to make a Cl_2 product. Reaction (10) provides a decomposition pathway for the Cl_2^- intermediate that produces CH_2ClI and I^- products that have been observed in the NMR and UV/VIS photochemistry experiments.

D. Discussion of the water catalyzed O−H insertion/HI elimination reactions and likely implications for decomposition of polyhalomethanes in water and salt water environments

The ultraviolet photolysis of CH_2I_2 in the gas phase primarily undergoes direct C–I bond cleavage to produce CH_2I radical and I atom photofragments with a near unity quantum yield.[24−26] However, we have observed that ultraviolet photolysis of low concentrations of CH_2I_2 in aqueous environments without salt present leads to conversion of the parent molecule into HI and $CH_2(OH)_2$ products with an appreciable photoquantum yield (Ref. 80). Corresponding ultraviolet photolysis of CH_2I_2 in salt water solutions also leads to conversion of the parent molecule mostly into HI and $CH_2(OH)_2$ products but also noticeable amounts of CH_2ICl and Cl_2^- species (this work). These results clearly indicate the ultraviolet photochemistry of CH_2I_2 displays substantial phase dependence with greatly different reactions taking place in aqueous environments compared to the gas phase.

The reaction mechanism elucidated in Ref. 80 and briefly discussed here in Sec. III C can account for how ultraviolet photolysis of CH_2I_2 in aqueous environments leads to appreciable production of HI and $CH_2(OH)_2$ products. We note the water catalyzed reactions of isopolyhalomethanes and their reaction products may be noticeable sources of halogens and/or strong acids in the natural environment and this phase dependent water solvated photochemistry has not yet been considered in modeling the photochemistry of polyhalomethanes in the natural environment.

CH_2I_2 and other polyhalomethanes such as CH_2IBr and CH_2ICl have been observed in sea water and in the marine boundary layer of the troposphere and their production attributed mostly to biogenic sources such as microalgae.[7,93,94] The measured surface sea water levels of CH_2I_2 and CH_2IBr were found to be lower than those computed from seaweed production and this is likely due to photodissociation in the water column.[93,94] However, the levels of CH_3I and CH_2ICl calculated from measured emission rates and biomass estimates could not account for the high levels of these species in surface coastal waters and this may be due to additional marine sources for these compounds.[93,94] Our present results for photolysis of CH_2I_2 in salt (NaCl) water with comparable salt concentrations as sea water found that noticeable amounts of CH_2ICl are produced (see NMR photochemistry results of Fig. 3). This would be a different marine source of CH_2ICl and can potentially account for the higher than expected levels of CH_2ICl found in surface coastal waters. Further work is needed to better estimate the actual contribution of this different photochemical route to formation of CH_2ICl in surface sea water. We note that the relatively intense absorption of CH_2I_2 at wavelengths longer than 300 nm in the sunlight region leads this molecule to have a very short lifetime in the natural environment since it is readily photodissociated. However, the CH_2ICl species has a substantially weaker absorption that is in the ultraviolet around 260 nm with very little absorption in the sunlight region. Thus, the CH_2ICl species would have a noticeably longer lifetime in the natural environment. This suggests that any CH_2ICl produced from photolysis of CH_2I_2 in sea water may still be discernible long after the disappearance of the precursor CH_2I_2 species. It would be interesting to examine the photolysis of CH_2I_2 in the natural environment and see if this correlates with noticeable formation of CH_2ICl in surface coastal waters. The formation of CH_2ICl could potentially serve as a marker for salt water photolysis of CH_2I_2 versus photolysis of CH_2I_2 in nonsalt water environments such as pure water or ice particles, or in the gas phase where CH_2ICl is likely not directly produced from photolysis of CH_2I_2.

Our present results and comparison of the ultraviolet photolysis of CH_2I_2 in nonsalt and salt aqueous environments also has some interesting implications for photolysis of polyhalomethanes in aqueous sea salt particles. At relatively low concentrations to moderate concentrations of salt comparable to sea water, there will still be significant formation of isopolyhalomethanes and their associated reactions with water to release strong acids (HX). Using CH_2I_2 as an example, the HI strong acid and methanediol $[CH_2(OH)_2]$ products produced by CH_2I_2 photolysis will be accompanied

by some formation of CH_2ICl and Cl_2^- products/intermediates produced from reactions of the initially formed CH_2I radical and I atom photofragments. As the salt concentration increases, it would be reasonable to expect that the production of strong acids and water catalyzed reactions will decrease and more products produced from reactions of the initially formed CH_2I radical and I photofragments with the salt (mainly NaCl) in the sea salt particle. Therefore the polyhalomethane photochemistry to produce strong acids and potential halogen activation will likely strongly vary with the level of water or salt in the aqueous sea salt particles. Much more work remains to be done by a number of research groups with a range of expertise to better understand the photochemistry and chemistry of polyhalomethanes in different types of aqueous solutions and in the natural environment. We anticipate this will become an increasing area of investigation.

IV. CONCLUSION

Photochemistry and ps-TR^3 experiments were done for the ultraviolet photolysis of CH_2I_2 in salt water solutions and compared to corresponding results done in aqueous solutions that contain no salt. We found that photolysis of CH_2I_2 in aqueous environments containing no salt and salt up to $0.5M$ NaCl produced mostly $CH_2(OH)_2$ and HI products. Ps-TR^3 experiments showed that CH_2I–I is produced within several picoseconds and appears to then react with water in salt and nonsalt aqueous environments. When CH_2I_2 undergoes photolysis in aqueous solutions containing salt, different products/intermediates were produced (CH_2ICl and Cl_2^-) and the amount of $CH_2(OH)_2$ and HI products appears to decrease compared to photolysis in nonsalt aqueous solutions. The products/intermediates (CH_2ICl and Cl_2^-) appear to be formed from reactions of the CH_2I radical and I atom photofragments initially produced after CH_2I_2 photolysis with other species. We briefly discuss possible implications for the photodissociation of CH_2I_2 and potentially other polyhalomethanes in the natural environment.

[1] Th. Class and K. Ballschmiter, J. Atmos. Chem. **6**, 35 (1988).
[2] S. Klick and K. Abrahamsson, J. Geophys. Res. **97**, 12683 (1992).
[3] K. G. Heumann, Anal. Chim. Acta **283**, 230 (1993).
[4] R. M. Moore, M. Webb, R. Tokarczyk, and R. Wever, J. Geophys. Res., [Oceans] **101**, 20899 (1996).
[5] C. T. McElroy, C. A. McLinden, and J. C. McConnell, Nature (London) **397**, 338 (1997).
[6] J. C. Mössinger, D. E. Shallcross, and R. A. Cox, J. Chem. Soc., Faraday Trans. **94**, 1391 (1998).
[7] L. J. Carpenter, W. T. Sturges, S. A. Penkett, and P. S. Liss, J. Geophys. Res., [Oceans] **104**, 1679 (1999).
[8] B. Alicke, K. Hebstreit, J. Stutz, and U. Platt, Nature (London) **397**, 572 (1999).
[9] R. P. Wayne, *Chemistry of Atmospheres*, 3rd ed. (Oxford University Press, Oxford, UK, 2000).
[10] S.-F. Fan and D. J. Jacob, Nature (London) **359**, 522 (1992).
[11] M. Mozurkewich, J. Geophys. Res. **100**, 14199 (1995).
[12] R. Vogt, P. J. Crutzen, and S. Sander, Nature (London) **383**, 327 (1996).
[13] R. Sander and P. J. Crutzen, J. Geophys. Res. **101**, 9121 (1996).
[14] K. W. Oum, M. J. Lakin, D. O. DeHaan, T. Brauers, and B. J. Finalyson-Pitts, Science **279**, 74 (1998).
[15] C. T. McElroy, C. A. McLinden, and J. C. McConnell, Nature (London) **397**, 338 (1999).
[16] R. Vogt, R. Sander, R. V. Glasow, and P. J. Crutzen, J. Atmos. Chem. **32**, 375 (1999).
[17] W. Behnke, M. Elend, U. Krüger, and C. Zetzsch, J. Atmos. Chem. **34**, 87 (1999).
[18] E. M. Knipping, M. J. Lakin, K. L. Foster, P. Jungwirth, D. J. Tobias, R. B. Gerber, D. Dabdub, and B. J. Finalyson-Pitts, Science **288**, 301 (2000).
[19] B. J. Finalyson-Pitts and J. C. Hemminger, J. Phys. Chem. A **104**, 11463 (2000).
[20] K. L. Foster, R. A. Plastridge, J. W. Bottenheim, P. B. Shepson, B. J. Finalyson-Pitts, and C. W. Spicer, Science **291**, 471 (2001).
[21] X.-Y. Yu and J. R. Barker, J. Phys. Chem. A **107**, 1313 (2003).
[22] K. Pfeilsticker, A. Lotter, C. Peters, and H. Bösch, Science **300**, 2078 (2003).
[23] M. E. Dunn, E. K. Pokon, and G. C. Shields, J. Am. Chem. Soc. **126**, 2647 (2004).
[24] M. Kawasaki, S. J. Lee, and R. Bersohn, J. Chem. Phys. **63**, 809 (1975).
[25] G. Schmitt and F. J. Comes, J. Photochem. **14**, 107 (1980).
[26] P. M. Kroger, P. C. Demou, and S. J. Riley, J. Chem. Phys. **65**, 1823 (1976).
[27] J. B. Koffend and S. R. Leone, Chem. Phys. Lett. **81**, 136 (1981).
[28] S. R. Cain, R. Hoffman, and R. Grant, J. Phys. Chem. **85**, 4046 (1981).
[29] S. J. Lee and R. Bersohn, J. Phys. Chem. **86**, 728 (1982).
[30] L. J. Butler, E. J. Hintsa, and Y. T. Lee, J. Chem. Phys. **84**, 4104 (1986).
[31] L. J. Butler, E. J. Hintsa, and Y. T. Lee, J. Chem. Phys. **86**, 2051 (1987).
[32] E. A. J. Wannenmacher, P. Felder, and J. R. Huber, J. Chem. Phys. **95**, 986 (1991).
[33] G. Baum, P. Felder, and J. R. Huber, J. Chem. Phys. **98**, 1999 (1993).
[34] U. Marvet and M. Dantus, Chem. Phys. Lett. **256**, 57 (1996).
[35] Q. Zhang, U. Marvet, and M. Dantus, J. Chem. Phys. **109**, 4428 (1998).
[36] K.-W. Jung, T. S. Ahmadi, and M. A. El-Sayed, Bull. Korean Chem. Soc. **18**, 1274 (1997).
[37] W. Radloff, P. Farmanara, V. Stert, E. Schreiber, and J. R. Huber, Chem. Phys. Lett. **291**, 173 (1998).
[38] K. Kavita and P. K. Das, J. Chem. Phys. **112**, 8426 (2000).
[39] S. L. Baughcum, H. Hafmann, S. R. Leone, and D. Nesbitt, Faraday Discuss. **67**, 306 (1979).
[40] S. L. Baughcum and S. R. Leone, J. Chem. Phys. **72**, 6531 (1980).
[41] G. Maier and H. P. Reisenauer, Angew. Chem., Int. Ed. Engl. **25**, 819 (1986).
[42] G. Maier, H. P. Reisenauer, J. Lu, L. J. Scaad, and B. A. Hess, Jr., J. Am. Chem. Soc. **112**, 5117 (1990).
[43] B. J. Schwartz, J. C. King, J. Z. Zhang, and C. B. Harris, Chem. Phys. Lett. **203**, 503 (1993).
[44] K. Saitow, Y. Naitoh, K. Tominaga, and Y. Yoshihara, Chem. Phys. Lett. **262**, 621 (1996).
[45] A. N. Tarnovsky, J.-L. Alvarez, A. P. Yartsev, V. Sündstrom, and E. Åkesson, Chem. Phys. Lett. **312**, 121 (1999).
[46] A. N. Tarnovsky, M. Wall, M. Rasmusson, T. Pascher, and E. Åkesson, J. Chin. Chem. Soc. (Taipei) **47**, 769 (2000).
[47] A. N. Tarnovsky, M. Wall, M. Gustafsson, N. Lascoux, V. Sundström, and E. Åkesson, J. Phys. Chem. A **106**, 5999 (2002).
[48] M. Wall, A. N. Tarnovsky, T. Pascher, V. Sundström, and E. Åkesson, J. Phys. Chem. A **107**, 211 (2003).
[49] W. M. Kwok, C. Ma, A. W. Parker, D. Phillips, M. Towrie, P. Matousek, and D. L. Phillips, J. Chem. Phys. **113**, 7471 (2000).
[50] X. Zheng and D. L. Phillips, Chem. Phys. Lett. **324**, 175 (2000).
[51] X. Zheng and D. L. Phillips, J. Chem. Phys. **113**, 3194 (2000).
[52] X. Zheng and D. L. Phillips, J. Phys. Chem. A **104**, 6880 (2000).
[53] X. Zheng, W. M. Kwok, and D. L. Phillips, J. Phys. Chem. A **104**, 10464 (2000).
[54] X. Zheng, W.-H. Fang, and D. L. Phillips, J. Chem. Phys. **113**, 10934 (2000).
[55] X. Zheng, C. W. Lee, Y.-L. Li, W.-H. Fang, and D. L. Phillips, J. Chem. Phys. **114**, 8347 (2001).
[56] W. M. Kwok, C. Ma, A. W. Parker, D. Phillips, M. Towrie, P. Matousek, X. Zheng, and D. L. Phillips, J. Chem. Phys. **114**, 7536 (2001).

[57] W. M. Kwok, C. Ma, A. W. Parker, D. Phillips, M. Towrie, P. Matousek, and D. L. Phillips, Chem. Phys. Lett. **341**, 292 (2001).

[58] Y.-L. Li, D. Wang, and D. L. Phillips, Bull. Chem. Soc. Jpn. **75**, 943 (2002).

[59] W. M. Kwok, C. Ma, A. W. Parker, D. Phillips, M. Towrie, P. Matousek, and D. L. Phillips, J. Phys. Chem. A **107**, 2624 (2003).

[60] D. L. Phillips, W.-H. Fang, and X. Zheng, J. Am. Chem. Soc. **123**, 4197 (2001).

[61] D. L. Phillips and W.-H. Fang, J. Org. Chem. **66**, 5890 (2001).

[62] Y.-L. Li, K. H. Leung, and D. L. Phillips, J. Phys. Chem. A **105**, 10621 (2001).

[63] W.-H. Fang, D. L. Phillips, D. Wang, and Y.-L. Li, J. Org. Chem. **67**, 154 (2002).

[64] Y.-L. Li, D. M. Chen, D. Wang, and D. L. Phillips, J. Org. Chem. **67**, 4228 (2002).

[65] Y.-L. Li, D. Wang, and D. L. Phillips, J. Chem. Phys. **117**, 7931 (2002).

[66] D. Wang, D. L. Phillips, and W.-H. Fang, Phys. Chem. Chem. Phys. **4**, 5059 (2002).

[67] D. L. Phillips, Curr. Org. Chem. **8**, 739 (2004).

[68] L. B. Harding, H. B. Schlegel, R. Krishnan, and J. A. Pople, J. Phys. Chem. **84**, 3394 (1980).

[69] J. A. Pople, K. Raghavachari, M. J. Frisch, J. B. Blinkley, and P. V. R. Schleyer, J. Am. Chem. Soc. **105**, 6389 (1983).

[70] C. Wesdemiotis, R. Feng, P. O. Danis, E. R. Williams, and F. W. Lafferty, J. Am. Chem. Soc. **108**, 5847 (1986).

[71] B. F. Yates, W. J. Bouma, and L. Radom, J. Am. Chem. Soc. **109**, 2250 (1987).

[72] W. Kirmse, T. Meinert, D. A. Moderelli, and M. S. Platz, J. Am. Chem. Soc. **115**, 8918 (1993).

[73] S. P. Walch, J. Chem. Phys. **98**, 3163 (1993).

[74] C. Gonzalez, A. Restrepo-Cossio, M. Márquez, and K. B. Wiberg, J. Am. Chem. Soc. **118**, 5408 (1996).

[75] C. J. Moody and G. H. Whitman, in *Reactive Intermediates*, edited by S. G. Davies (Oxford University Press, New York, 1992).

[76] J. R. Pliego, Jr. and W. B. De Almeida, J. Phys. Chem. **100**, 12410 (1996).

[77] J. R. Pliego, Jr. and W. B. De Almeida, J. Phys. Chem. A **103**, 3904 (1999).

[78] W. M. Kwok, C. Zhao, Y.-L. Li, X. Guan, and D. L. Phillips, J. Chem. Phys. **120**, 3323 (2004).

[79] W. M. Kwok, C. Zhao, Y.-L. Li, X. Guan, D. Wang, and D. L. Phillips, J. Am. Chem. Soc. **126**, 3119 (2004).

[80] W. M. Kwok, C. Zhao, X. Guan, Y. L. Li, Yong Du, and D. L. Phillips, J. Chem. Phys. **120**, 9017 (2004).

[81] A. J. Hynes and P. H. Wine, J. Chem. Phys. **89**, 3565 (1988).

[82] A. N. Tarnovsky, V. Sundstrom, E. Akesson, and T. Pascher, J. Phys. Chem. A **108**, 237 (2004).

[83] Y.-L. Li, C. Zhao, W. M. Kwok, X. Guan, P. Zuo, and D. L. Phillips, J. Chem. Phys. **119**, 4671 (2003).

[84] R. Wilbrandt, N. H. Jensen, A. H. Sillensen, and K. B. Hansen, Chem. Phys. Lett. **106**, 503 (1984).

[85] G. N. R. Tripathi, R. H. Schuler, and R. W. Fessenden, Chem. Phys. Lett. **113**, 563 (1985).

[86] G. S. Tyndall, T. J. Wallington, M. D. Hurley, and W. F. Schneider, J. Phys. Chem. **97**, 1576 (1993).

[87] T. J. Wallington, W. F. Schneider, I. Barnes, K. H. Becker, J. Sehested, and O. J. Nielsen, Chem. Phys. Lett. **322**, 97 (2000).

[88] H. Knuttu, M. Dahlqvist, J. Murto, and M. Räsänen, J. Phys. Chem. **92**, 1495 (1988).

[89] D. J. Le Botlan, B. J. Mechin, and G. J. Martin, Anal. Chem. **55**, 587 (1983).

[90] R. P. Bell, Adv. Phys. Org. Chem. **4**, 1 (1966).

[91] A. A. Zavitsas, M. Coffiner, T. Wiseman, and L. R. Zavitsas, J. Phys. Chem. **74**, 2746 (1970).

[92] X.-Y. Yu, Z.-C. Bao, and J. R. Barker, J. Phys. Chem. A **108**, 295 (2004).

[93] L. J. Carpenter, G. Malin, F. Kuepper, and P. S. Liss, Global Biogeochem. Cycles **14**, 1191 (2000).

[94] L. J. Carpenter, Chem. Rev. (Washington, D.C.) **103**, 4953 (2003).